

Manuscript Number: JALCOM-D-15-09601R1

Title: Acetone Sensors Based on TiO<sub>2</sub> Nanocrystals Modified with Tungsten Oxide Species

Article Type: Full Length Article

Keywords: nanocrystalline TiO<sub>2</sub>; chemical synthesis; sol-gel process; gas-sensor; electrical conductivity.

Corresponding Author: Dr. Mauro Epifani,

Corresponding Author's Institution: Consiglio Nazionale delle Ricerche (IMM-CNR)

First Author: Mauro Epifani

Order of Authors: Mauro Epifani; Elisabetta Comini; Raúl Díaz; Aziz Genç; Teresa Andreu; Pietro Siciliano; Joan R Morante

Abstract: TiO<sub>2</sub> nanocrystals were prepared by sol-gel/ solvothermal processing and modified by the addition of W precursor before the solvothermal step. The W : Ti nominal atomic ratio (RW) was fixed to 0.16 and 0.64. Surface modification of TiO<sub>2</sub> occurred for RW = 0.16 while for RW = 0.64 nanocomposites with WO<sub>3</sub> nanocrystals were obtained after heat-treatment at 500 °C. Pure TiO<sub>2</sub> proved to be very poorly performing in acetone sensing in all the operating conditions. Instead, the addition of both W concentrations largely enhanced the sensor response. It ranged over two orders of magnitude of conductance variation for all the tested concentrations at as low as 200 °C operating temperature. The results showed that it is possible to enhance the performance of an otherwise almost inactive oxide like TiO<sub>2</sub> by proper combination with another more active oxide like WO<sub>3</sub>.

## Novelty statement

The search for novel materials nanoarchitectures and the consequently stemming new physico-chemical properties encompasses an enormously increasing range of compositions and typologies. Among these, many less efforts have been devoted to coupled metal oxides. One can find few examples concerning vapour deposition techniques, and other few works by application of SILAR methods. A careful investigation of the application of colloidal syntheses must still be developed, and it would give access to a broad range of materials with important base properties to be coupled with the surface activation. In this work we present the acetone sensing properties of the colloidal version of the  $\text{TiO}_2\text{-WO}_3$  system. While deeply explored in many applications, it can be found that the  $\text{TiO}_2$  base materials used in other  $\text{TiO}_2\text{-WO}_3$  related works usually have bulk properties, being obtained commercially or by precipitation. In this paper, we have exploited the synthesis of colloidal  $\text{TiO}_2$  nanocrystals by a procedure that allows to co-grow  $\text{WO}_x$  species during the solvothermal synthesis of  $\text{TiO}_2$ . We show that the use of nanocrystalline  $\text{TiO}_2$  base material, and of a suitable W precursor, allows achieving a whole range of materials architectures, ranging from  $\text{WO}_x$  surface modified  $\text{TiO}_2$  to its whole wrapping by  $\text{WO}_x$  amorphous gel. What we obtain is a fully nanosized version of the  $\text{TiO}_2\text{-WO}_3$  system, which is made possible by the comparable sizes of the  $\text{TiO}_2$  and  $\text{WO}_3$  components. We show that the surface modification of  $\text{TiO}_2$  triggers its surface chemistry by enhancing the acetone oxidation capability by two orders of magnitude with respect to naked titania. We believe that this work extends the range of available surface active materials by a rational approach conducted by the comparison with heterogeneous catalysis. These results fully complement the ones that we already obtained for ethanol, reinforcing the view of surface catalytic activation by foreign oxide species, and the concept of novel material architecture different from pure core-shell structure.



Consiglio Nazionale delle Ricerche

## ISTITUTO PER LA MICROELETTRONICA E I MICROSISTEMI

Lecce University Campus - Via Arnesano - 73100 Lecce (Italy)  
Tel: (39-0832)-422502 - Direction (39-0832) -422500  
VAT N. 02118311006

---

Lecce, 8 January 2016

**Prof. K.H. Jürgen Buschow**  
**Editor**  
**Journal of Alloys and Compounds**

**Subject:** submission of **revised** manuscript JALCOM-D-15-09601 for publication in **Journal of Alloys and Compounds**

Dear Editor,

Thank you for giving us the possibility of considering the reviewer's indications. The answers to the reviewer's queries are reported below. The related changes in the manuscript have been highlighted in yellow.

*The detailed comments are:*

*“There are some grammatical and spelling errors including the lack of preposition and the inappropriate use of word and active voice. Some sentences are too long.”*

Auhors' reply: in the new manuscript, we have strived to polish the language as carefully as possible.

*“Figure 4, it seem that pure WO<sub>3</sub> showed the higher response than W modified TiO<sub>2</sub> at 200°C, while the similar response value was also obtained at other temperature (below 350°C ). Therefore some sentences and references should be added to clearly understand why TiO<sub>2</sub> was selected as sensing materials. By the way, TiO<sub>2</sub> are a very interesting photocatalyst material.”*

Auhors' reply: actually, we were not pushed to study the modification of TiO<sub>2</sub> by its *photo*-catalytic properties, but this study is a part of a program where we are investigating the sensing properties of materials that are well-known as heterogeneous catalysts. Many of these systems are TiO<sub>2</sub> supported metal oxides. The first system that we considered was TiO<sub>2</sub>-V<sub>2</sub>O<sub>5</sub> and, encouraged by the related results, we continued the investigation with another known catalyst system like TiO<sub>2</sub>-WO<sub>3</sub>. The fact that TiO<sub>2</sub> has, by itself, a poor response just enhanced the importance of the surface modification. We have inserted the data related to WO<sub>3</sub> just for showing how effective is the



Consiglio Nazionale delle Ricerche

## ISTITUTO PER LA MICROELETTRONICA E I MICROSISTEMI

Lecce University Campus - Via Arnesano - 73100 Lecce (Italy)  
Tel: (39-0832)-422502 - Direction (39-0832) -422500  
VAT N. 02118311006

---

Lecce, 8 January 2016

surface modification since, by just “painting” the surface of anatase with the  $WO_x$  layers, the response of  $TiO_2$  is triggered to values comparable to pure  $WO_3$ , which is a powerful acetone sensor. We have included these considerations in the new version of the manuscript.

*”Authors investigated the effect of W content on the sensing properties. However, only two kind of sample were investigated. As a full length paper, it will be more interesting if other W: Ti nominal atomic ratio was investigated and added in this paper.”*

Auhors’ reply: in the paper devoted to the study of the synthesis process and of the related materials characterization, we indeed considered different intermediate W concentrations between the two shown in the present manuscript. The XRD patterns suggested that there were no peculiar structural differences with the  $R_{0.64}$  sample. For this reason, and for simplifying the overwhelmingly hard characterization work needed to elucidate the materials structure, we decided to focus onto the two extreme compositions. The related sensing results showed, a posteriori, that indeed the two chosen composition are representative of the overall sensing trends.

*”Authors focused on the acetone sensing properties in this paper, while ethanol sensing properties was invested in other paper. In this study, it can be seen that acetone sensing response was higher than ethanol. Could you explain why it behaves in that way?”*

Auhors’ reply: there are not many mechanistic studies, above all as concerns the reactions with ethanol and acetone, and even less if we consider a  $WO_3$  substrate. However, for ethanol sensing on  $SnO_2$  its adsorption followed by concurrent formaldehyde and hydrogen desorption had been suggested (Kohl et al.), while for acetone sensing the production of only  $CO_2$  and water has been recorded. These results point to very different reaction mechanisms, in turn triggered by the presence of an OH group in ethanol, differently from acetone. Acetone adsorption onto the oxygen defective  $WO_x$  surfaces could be more favored than that of ethanol, where the presence of an hydrogen atom bonded to oxygen may result in different electronic distribution and steric hindrance. Of course this is not an explanation, in the presence knowledge status, but it can be regarded as a



Consiglio Nazionale delle Ricerche

## ISTITUTO PER LA MICROELETTRONICA E I MICROSISTEMI

Lecce University Campus - Via Arnesano - 73100 Lecce (Italy)  
Tel: (39-0832)-422502 - Direction (39-0832) -422500  
VAT N. 02118311006

---

Lecce, 8 January 2016

useful starting point for further mechanistic studies. Since it is still at a speculative step, we have not included this view in the paper. If the referee judges that it would be more appropriate to displace it to the manuscript, we will add this part.

*"Authors explained the sensing performance by the surface modification and heterojunction. Could you comment it in a more detailed way? Some theory should be added to clearly declare it within the body text."*

Auhors' reply: a paragraph has been added at the end of the discussion with additional hypotheses and considerations.

*"The characterization of the materials has been investigated in other paper. However, it is better to add SEM and TEM images to understand the morphology of product."*

Auhors' reply: we have added some new TEM images. The SEM images would not be useful since the materials, after the heat-treatment, are constituted by aggregated nanocrystals, and despite they keep a size below 10 nm, only by HRTEM a clearly discernible morphology is obtained.

*"For practical applications, the gas sensing stability of the sensor device is a very important parameter. For this reason, the fabricated gas sensor with synthesized sensing materials should be tested during long period, for instance, more than 1 month."*

Auhors' reply: the referee is right, indeed we carry out some standard tests on the devices, in the synthesis paper we reported "The sensing devices selected for the gas tests had base conductance values dispersed within 10% of the results showed in the manuscript. In this case, the measured responses were also comprised in such range. Error bars were hence not included in the plots for clarity sake. Repeated experiments under the same operational conditions yielded stable and reproducible sensor responses for several months (estimated uncertainty =  $\pm 10\%$ )."

This is quite a standard result that we have obtained for many different systems. In the manuscript we have reported the last sentence.



Consiglio Nazionale delle Ricerche

## ISTITUTO PER LA MICROELETTRONICA E I MICROSISTEMI

Lecce University Campus - Via Arnesano - 73100 Lecce (Italy)  
Tel: (39-0832)-422502 - Direction (39-0832) -422500  
VAT N. 02118311006

---

Lecce, 8 January 2016

*"p. 7 the concentration of acetone should be added in the body text."*

Auhors' reply: it has been added in page 7 of the current version of the manuscript.

*"p. 10 a table to summarize the performance of acetone gas sensor for metal oxide composite will be helpful to the readers. The result in this study should be compared with those reports and added in the table."*

Auhors' reply: the suggested table has been added.

*"p. 17 the title of figure 2 and 3, "working temperature" should be changed to "operating temperature"."*

Auhors' reply: thank you, it has been revised.

Best regards  
Mauro Epifani

# Acetone Sensors Based on TiO<sub>2</sub> Nanocrystals Modified with Tungsten Oxide

## Species

Mauro Epifani<sup>a,\*</sup>, Elisabetta Comini<sup>b</sup>, Raúl Díaz<sup>c</sup>, Aziz Genç<sup>d</sup>, Teresa Andreu<sup>e</sup>, Pietro Siciliano<sup>a</sup>, Joan R. Morante<sup>e,f</sup>

<sup>a</sup>Consiglio Nazionale delle Ricerche – Istituto per la Microelettronica e Microsistemi (CNR-IMM), via Monteroni c/o Campus Universitario, I-73100, Lecce (Italy);

<sup>b</sup>SENSOR Lab, Department of Information Engineering, Brescia University and CNR-INO, via Valotti, 9, 25133 Brescia, Italy;

<sup>c</sup>Electrochemical Processes Unit, IMDEA Energy Institute, Avda. Ramón de la Sagra, 3 28935 Móstoles, Spain

<sup>d</sup>Metallurgy and Materials Engineering Department, Faculty of Engineering, Bartın University, 74100, Bartın, Turkey

<sup>e</sup>Catalonia Institute for Energy Research- (IREC), Jardíns de les Dones de Negre, 1, E-08930 Sant Adrià del Besos, Barcelona, CAT, Spain;

<sup>f</sup>Departament d'Electrònica, Universitat de Barcelona, C.\ Martí i Franquès 1, E-08028 Barcelona, Spain

\*[mauro.epifani@le.imm.cnr.it](mailto:mauro.epifani@le.imm.cnr.it), phone: +39 0832 299775

## **Abstract**

TiO<sub>2</sub> nanocrystals were prepared by sol-gel/ solvothermal processing and modified by the addition of W precursor before the solvothermal step. The W : Ti nominal atomic ratio ( $R_W$ ) was fixed to 0.16 and 0.64. Surface modification of TiO<sub>2</sub> occurred for  $R_W = 0.16$  while for  $R_W = 0.64$  nanocomposites with WO<sub>3</sub> nanocrystals were obtained after heat-treatment at 500 °C. Pure TiO<sub>2</sub> proved to be very poorly performing in acetone sensing in all the operating conditions. Instead, the addition of both W concentrations largely enhanced the sensor response. It ranged over two orders of magnitude of conductance variation for all the tested concentrations at as low as 200 °C operating temperature. The results showed that it is possible to enhance the performance of an otherwise almost inactive oxide like TiO<sub>2</sub> by proper combination with another more active oxide like WO<sub>3</sub>.

**Keywords:** nanocrystalline TiO<sub>2</sub>; chemical synthesis; sol-gel process; gas-sensor; electrical conductivity.

## 1. Introduction

Metal oxide heterojunctions have been long-time known as an interesting alternative to modify the sensing performances of single oxides [1]. Relevant examples include  $\text{TiO}_2\text{-SnO}_2$  [2, 3],  $\text{MoO}_3\text{-WO}_3$  [4],  $\text{SnO}_2\text{-ZnO}$  [5-8] and  $\text{TiO}_2\text{-WO}_3$  [9-13]. In the context of gas sensors, by heterojunction we mean the co-existence of different oxide grains exposed to the gaseous analyte, so we have excluded from our considerations the recent works on core-shell structures grown by various methods [14]. The interest for such systems stems from the hypothesized improvement of the sensing performances due to the combination of the electronic features of the component oxides. But it is not clear what should be meant by “combination” which instead is better defined in photocatalytic and photoelectrochemical systems, and relies on the band alignment of the two oxide components. Moreover, the comparison of the performance of the composite materials with the single components, for verifying the effectiveness of the nanocomposites formation, has been very scarcely investigated [7]. In a program where we are investigating the sensing properties of well-known heterogeneous catalysts, we realized that many of these systems are  $\text{TiO}_2$  supported metal oxides. Hence, they well fit to the above described interest for metal oxide heterojunctions. In this context, we recently introduced [15] a chemical route for the synthesis of  $\text{TiO}_2\text{-WO}_3$  nanocomposites. By controlling the chemical properties of the precursors (in particular, the hydrolytic reactivity) and the W concentration, we could prepare a range of structures ranging from  $\text{TiO}_2$  anatase nanocrystals modified by a monolayer of W oxide, to heterojunctions constituted by  $\text{WO}_3$  nanocrystallites dispersed into the anatase host. The nanocomposites exhibited remarkably improved ethanol sensing properties with respect to pure  $\text{TiO}_2$ , which was interpreted mainly as an effect of the surface modification by  $\text{WO}_x$  species. For enhancing this interpretation, here we show complete acetone [16] sensing tests carried out onto the  $\text{WO}_x$  modified materials and the pure oxide components, for comparison. We show that interaction of the two oxides remarkably enhances the sensor response with respect to pure  $\text{TiO}_2$ , and just monolayers of W oxides are sufficient to reach the performances of pure  $\text{WO}_3$ . On the basis of these results, at the end of the paper we will briefly re-

consider the concept of heterojunctions in gas sensing field. Hence, the concept of “combination” of the electronic features depends on the kind of structures present in the final material.

## 2. Experimental

For preparing TiO<sub>2</sub>-WO<sub>3</sub> composite structures, we adopted the following procedure [15]. First, TiO<sub>2</sub> amorphous nanoparticles were prepared by reaction of 2 mL of Ti precursor solution in 10 mL of dodecylamine at 100 °C for 1 hour into a glass vial. The white precipitate was extracted with methanol and washed three times in acetone. The Ti precursor solution was prepared by methanolysis of 0.75 g of TiCl<sub>4</sub> in 10 mL of methanol, followed by the addition of 1.2 mL of water [17]. Then, the obtained amorphous TiO<sub>2</sub> nanoparticles were crystallized by solvothermal processing into a teflon lined steel autoclave, after being dispersed in 10 mL of oleic acid. Then, a controlled amount of tungsten chloro-alkoxide was added to the TiO<sub>2</sub> dispersion [18]. W : Ti nominal atomic ratios (R<sub>w</sub>) of 0.16 and 0.64 were used. The W chloro-alkoxide was prepared from WCl<sub>6</sub> as previously described [18]. The solvothermal step was then carried out for 2 h at 250 °C. After the solvothermal step, the nanocrystals were extracted with methanol, washed in acetone and dried at 90 °C. Then, they were heat-treated up to 500 °C for organics elimination and thermal stabilization. The gas-sensing tests were carried out using a standard configuration for resistive sensor measurement, with Pt interdigitated (ID) electrodes and a Pt heater deposited onto an alumina substrate (size of the single device: 2x2 mm<sup>2</sup>). Sensors were fabricated by depositing onto the just described substrates a paste made by mixing the 500 °C TiO<sub>2</sub>-WO<sub>3</sub> nanocrystals with 1,2-propanediol. Before measurements, the sensors were kept at a temperature of 400 °C, provided by the sensor heaters, in order to decompose the organic residuals and stabilize the electrical signal. For this aim, and for sensing tests, the sensor devices were placed in a sealed chamber with a constant flux of 0.3 L/min of humid synthetic air (79%N<sub>2</sub> - 21%O<sub>2</sub>, 40%RH @20°C) into which the desired amount of acetone was mixed, in concentrations ranging from 50 to 500 ppm. The sensor response was defined as  $G-G_0/G_0$ , where G was the electrical conductance after equilibration with acetone and G<sub>0</sub> the equilibrium conductance before introduction of the gas into the test cell. The sensing

devices selected for the gas tests had base conductance values within 10% of the results showed in the manuscript. Repeated experiments under the same operational conditions yielded stable and reproducible sensor responses for several months (estimated uncertainty =  $\pm 10\%$ ). For completing the picture of the sensing improvement with respect to pure TiO<sub>2</sub>, responses to other gases will be shown at the end of the manuscript.

High resolution transmission electron microscopy (HRTEM) analyses were carried out with a field emission gun microscope FEI Tecnai F20, working at 200 kV and with a point-to-point resolution of 0.19 nm.

### 3. Results and discussion

As stated in the introduction, the synthesis of the materials had been previously investigated in detail, with particular stress onto the interaction of the Ti and W oxide species [15]. Here will report a summary of the main results, as guidance for differentiating the material structure depending on the W concentration. The XRD patterns of the nanocrystals heat-treated in different conditions [16, 19] are reported in the supplementary information for convenience of the reader. The patterns of the materials heat-treated up to 400 °C only displayed the anatase structure for  $R_W = 0.16$ . For  $R_W = 0.64$ , they additionally displayed very broad peaks in the same position of bulk WO<sub>3</sub>, suggesting the presence of amorphous WO<sub>x</sub> species. After heating at 500 °C, for  $R_W = 0.16$  no other phases were observed, while for  $R_W = 0.64$  the peaks of monoclinic WO<sub>3</sub> appeared, overlapped to the TiO<sub>2</sub> structure. Moreover, the TiO<sub>2</sub> peaks were shifted with respect to pure TiO<sub>2</sub>. These results were coupled with different other characterization techniques [15], whose main results are summarized in Table 1 for convenience of the reader. Overall, the results suggested the following hypotheses about the materials structure, also summarized in Table 1: for  $R_W = 0.16$  the as-prepared material was constituted by anatase TiO<sub>2</sub> nanocrystals, onto which WO<sub>x</sub> species were deposited as surface layer(s); further heat-treatment did not favor phase separation of WO<sub>3</sub>. It was a strong indication that separate W-containing species were *not* contained in the as-prepared material. For  $R_W = 0.64$ , phase separation of WO<sub>3</sub> nanocrystals occurred

after heating at 500 °C. It was concluded that a threshold concentration existed after which the W precursor forms separate species instead of being deposited onto TiO<sub>2</sub>. During the heat-treatment at 500 °C, these WO<sub>3</sub> species grow and/or improve their crystalline order, giving rise to more intense XRD signal, while part of tungsten migrates into the TiO<sub>2</sub> structure, causing the observed XRD peak shift and distortion of the Raman signal (see Table 1). We will come back to this observation when discussing the electrical data obtained during the sensing tests.

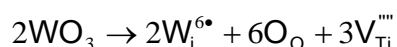
The difference between the structure of the R<sub>W</sub> = 0.16 and R<sub>W</sub> = 0.64 samples stems from the peculiar hydrolytic behavior of the W chloroalkoxide precursor. Precipitation in the related solution was observed after only a few weeks from the synthesis. No water could be used in the synthesis, and acetylacetone was added as a stabilizer. The W chloroalkoxide molecules hence show high affinity for self cross-linking. For low W concentration (R<sub>W</sub> = 0.16), W cross-linking still preferentially occurs with the surface of anatase, and we do not observe any phase separation of W oxides. When the W concentration increases (R<sub>W</sub> = 0.64), the probability that the W chloroalkoxide molecules self cross-link increases, which results in the gel structure enwrapping the anatase nanocrystals and the subsequent phase segregation of WO<sub>3</sub>. This is the base for the different structures obtained depending on the W concentration.

Transmission electron microscopy was used to gain more details about the structure of the samples. Figure 1 shows representative HRTEM images of the samples with R<sub>W</sub> = 0.16 and R<sub>W</sub> = 0.64, after heat-treatment at 500 °C. Despite the thermal elimination of the organic capping layer, it was still possible to distinguish single crystals of TiO<sub>2</sub> with a mean size of about 8 nm for R<sub>W</sub> = 0.16. The analysis of the power spectrum of various nanocrystals showed that there were no differences with the lattice parameters of anatase TiO<sub>2</sub> (lattice parameters a = b = 0.3785 nm and c = 0.9514 nm). For the sample with R<sub>W</sub> = 0.64, it was surprisingly not possible to detect WO<sub>3</sub> crystallites, whose presence was only ensured by XRD. Possible explanation is that the WO<sub>3</sub> species were intimately mixed with the TiO<sub>2</sub> host, due to the heat-treatment and the disappearance of the organic capping, making it very hard to

distinguish them in the material mass. In this case, the mean nanocrystals size was 10 nm. Instead, while the lattice parameters could still be attributed to anatase TiO<sub>2</sub>, there was a 3% uncertainty in their value, in agreement with the shift of the XRD patterns with respect to pure TiO<sub>2</sub>.

As explained in the introduction, our main aim was to test these peculiar structures toward acetone, for confirming the powerful interaction of our composite materials with reducing gases. We remind here that the devices were processed with the materials heat-treated at 500 °C, and that the tested concentrations ranged from 50 to 500 ppm.

Figure 2 shows representative dynamic response curves at an operating temperature of 250 °C. For showing the activating effect of the WO<sub>x</sub> modification on pure TiO<sub>2</sub>, the response of pure WO<sub>3</sub> sensors is also included. The WO<sub>3</sub> nanocrystals were prepared similarly to pure TiO<sub>2</sub>, with the W precursor described in the experimental section [19]. The curves show various interesting features. The pure materials featured remarkably different conductance behavior. The pure WO<sub>3</sub> baseline was almost 4 orders of magnitude larger than pure TiO<sub>2</sub>. In fact, it has been proposed that WO<sub>3</sub> electrical properties are dominated by oxygen vacancies [20], differently from pure TiO<sub>2</sub>. The R<sub>W</sub> = 0.16 sensor displayed the lowest conductance values. Instead, the sample with R<sub>W</sub> = 0.64 had a conductance systematically almost two orders of magnitude larger than pure TiO<sub>2</sub>. This fact was interpreted as follows. The substitutional incorporation of W<sup>6+</sup> cations into the tetragonal anatase lattice is favored by its effective ionic radius (coordination number 6), 0.060 nm, against the 0.0605 nm of Ti<sup>4+</sup> [21]. Moreover, the incorporation equations in Kröger-Vink notation are the following, for substitutional and interstitial WO<sub>3</sub> incorporation, respectively:



where W<sub>Ti</sub> and W<sub>i</sub> indicate substitutional and interstitial W(VI) ions, V<sub>Ti</sub> is a Ti vacancy, and O<sub>O</sub> an oxygen ion in regular lattice site. The incorporation in interstitial sites would require the creation of

three oxygen vacancies, which is much more unfavorable, from a structural and energy point of view, with respect to the single vacancy created for substitutional tungsten. The two extra electrons by each substitutional tungsten may be ionized to the conduction band, giving rise to the observed increase of the electrical conductance with respect to pure  $\text{TiO}_2$ . The presence of substitutional tungsten would also explain the XRD peak shift described above for  $R_W = 0.64$ . The fact that for  $R_W = 0.16$  the conductance is even lower than pure  $\text{TiO}_2$ , and the less remarked XRD peak shift with respect to  $R_W = 0.64$  show that the tungsten incorporation is a phenomenon that becomes more and more important with increasing its concentration.

Second, the pure  $\text{TiO}_2$  curve displayed so weak changes upon injection of acetone to appear almost completely flat in the plot scale. Instead, the other materials were remarkably affected by reaction with acetone. The response time was of the order of a few minutes, but it can be noted that the recovery requires longer times, ranging around 40 min. This phenomenon occurred for all the materials and suggested that the final adsorbed species could be the same regardless the investigated sensor. The presence of rooted carboxylate species could be responsible for so long recovery times. Finally, the most remarkable result: the response switches from that of almost inactive pure  $\text{TiO}_2$  to values comparable to those of pure  $\text{WO}_3$  by the addition of the lowest W concentration ( $R_W = 0.16$ ). In this case, we have seen that there are no discrete  $\text{WO}_3$  particles in the final materials, but only surface layers of  $\text{WO}_x$ . We have inserted the data related to  $\text{WO}_3$  just for showing how effective is the surface modification since, by just “painting” the surface of anatase with the  $\text{WO}_x$  layers, the response of  $\text{TiO}_2$  is triggered to values comparable to pure  $\text{WO}_3$ , which is a powerful acetone sensor.

These considerations appear more clearly when observing the calibration curves, as plotted in Figure 3 for two different operating temperatures. At 250 °C all the W containing materials (including pure  $\text{WO}_3$ ), provided similar responses, which were remarkably high and ranged over more than two orders of magnitude of conductance variation. Pure  $\text{TiO}_2$  was hugely outperformed by the other materials.

At a temperature of 400 °C, which more deeply affects the adsorption phenomena, the calibration curves showed a more varied behavior with respect to 250 °C, but the main features were preserved. Above all, the responses of the W-containing materials again outperformed pure TiO<sub>2</sub>. This time, pure WO<sub>3</sub> has an even lower response than the TiO<sub>2</sub>-WO<sub>3</sub> sensors, for all the investigated acetone concentrations. The powerful activating effect of W oxide species is evident if we consider the summary of the response to 100 ppm of acetone at various operating temperatures, as shown in Figure 4. On one hand, pure TiO<sub>2</sub> needs increasingly high operating temperatures for providing an observable response, and the response-temperature curve maximum was clearly shifted to extreme operating conditions. The TiO<sub>2</sub>-WO<sub>3</sub> sensors readily provided the maximum response at the lowest operating temperatures, and they outperformed or remained comparable to pure WO<sub>3</sub>. The last had a clear response trend, which seems fitted by a bell shaped curve peaked at low temperatures. Instead, the TiO<sub>2</sub>-WO<sub>3</sub> sensors have a flatter behavior, with high responses over a broad range of operating temperatures.

From the data shown until now, some considerations can be drawn. It is clear, first of all, that full understanding of the operation of the TiO<sub>2</sub>-WO<sub>3</sub> sensors requires a thorough investigation of their structure, for understanding where and how tungsten is placed. Nevertheless, the aim of the WO<sub>3</sub> combination with the TiO<sub>2</sub> core was completely achieved. For  $R_W = 0.16$ , in which no separate WO<sub>3</sub> species were obtained even after heat-treatment at 500 °C, the titania host material was triggered to an acetone response as high as two orders of magnitude of conductance variation. Just when this response was achieved, already at 200 °C, pure TiO<sub>2</sub> was still simply inactive. Similar responses were obtained for both  $R_W$  values. As explained above, for  $R_W = 0.64$  a particularly complex situation occurs, given by the coexistence of surface modified TiO<sub>2</sub> and separate WO<sub>3</sub>. The WO<sub>3</sub> crystallites influence the conduction processes, raising the value of the base current with respect to pure TiO<sub>2</sub>. On the other hand, the  $R_W = 0.16$  sensor had a current lower than pure TiO<sub>2</sub>. We can then conclude that the WO<sub>3</sub> crystallites had mainly the effect of enhancing the material conductance, but the sensing properties mainly depended on the surface modification of TiO<sub>2</sub>. Of course, the WO<sub>3</sub> crystallites do contribute to the

sensing process, but it is not a dominating process. The mechanistic explanation of the sensing enhancement by the surface  $\text{WO}_x$  species is still an unexplored topic. As stated above, only the precise determination of the W distribution may help in solving such a question.

The observation of response patterns at different temperatures confirmed the effectiveness of the surface modification for improving the adsorption properties and surface chemistry of pure  $\text{TiO}_2$ . Additional response data are shown in Figure 5. First of all, the materials show an appreciable tendency to detect acetone with respect to a similar gas (as concerns the sensing mechanisms) like ethanol. For the same concentration, the acetone response is ten times higher than for ethanol. Of course, it is not possible to suppress the ethanol response while keeping a high acetone response. For having a  $\text{NO}_2$  response comparable at least to ethanol, a 5 ppm concentration had to be used. This was in agreement with the oxidation properties of  $\text{TiO}_2$ - $\text{WO}_3$  catalysts, which made them suitable for detecting reducing gases. On the other hand, the  $\text{NO}_2$  response of the  $\text{TiO}_2$ - $\text{WO}_3$  materials is much higher than pure  $\text{TiO}_2$ , indicating that the surface  $\text{WO}_x$  deposition is effective in improving the overall adsorption properties of the materials. As expected, increasing the operating temperature reduces the  $\text{NO}_2$  response, due to less favored gas adsorption. In the case of  $\text{H}_2$ , which is characterized by different sensing mechanisms with respect to acetone and ethanol, a 500 ppm concentration was necessary for having results comparable with at least ethanol. On the other hand, it was appreciable that the W-modified sensors could detect remarkably low hydrogen concentrations. For all gases, the W addition had the same effect of boosting the response to values comparable to those of pure  $\text{WO}_3$ , again confirming the importance of surface modification of pure  $\text{TiO}_2$ . Moreover, the best operating temperature was lowered to 200 °C, indicating the improved catalytic/adsorption properties of the modified materials.

There are very few studies about the gas-sensing properties of  $\text{TiO}_2$ - $\text{WO}_3$  composite systems. Su et al. [13] prepared  $\text{TiO}_2$ - $\text{WO}_3$  nanocrystals with different W concentrations, and used them as benzene and other aromatic molecules sensors. As usual with these analytes, quite high operating temperatures were needed for obtaining appreciable responses. Other applications include humidity [11, 22] and  $\text{SO}_2$

sensors, in combination with  $V_2O_5$  [23]. It may be of interest to compare the present results with the activating effect observed in other recent works concerning acetone sensing. Recent examples include ZnO-CuO inverse opals [24], Nd-doped porous  $\alpha$ - $Fe_2O_3$  nanotubes [25], hierarchical nanostructured  $WO_3$ - $SnO_2$  materials [26],  $\alpha$ - $Fe_2O_3$ -ZnO-Au nanocomposites [27],  $In_2O_3$ - $WO_3$  heterojunction nanofibers [28],  $Fe_3O_4@Co_3O_4$  core-shell microspheres [29]. In comparison with these works, the materials that we have been synthesizing displayed largely outperforming responses, as shown by the comparison in Table 2. The meaning of this finding is not to set-up any kind of record, but to further highlight the sense to give to the term “nanocomposites” or “heterojunctions”. Our materials, at least for  $R_w = 0.16$ , are not heterojunctions or nanocomposites, nevertheless a strong cooperative effect is visible among the surface modification and the underlying anatase base material. Hence, we will spend some more words about this point.

On the basis of the above discussion, the preferred configuration in our materials seems to be the surface modification with respect to the heterojunctions. The gas responses were comparable for both  $R_w$  values, but the surface modification has the advantage of employing less tungsten but, above all, to avoid the formation of heterojunctions. Heterojunctions are anyway inhomogeneous, despite on a nanometer scale: the  $WO_3$  crystallites seem evenly distributed and from TEM there is no evidence of accumulation regions. Nevertheless, local phase separations may negatively affect the long term stability of the sensor. The choice between surface modification and heterojunction has been based only on operational considerations. Both situations are worth deeper investigation since, as described above, different sensing mechanisms seem to be operative at the various operating temperatures and the investigation of the heterojunction behavior appears as an attractive topic by itself.

It appears that in real heterojunctions (i.e., co-existence of different oxides) each component is acting independently with its own sensing properties Overall conductance is generated by charge transport through the different grains. In this case, “combination” of the properties of the two oxides may be quite a weak concept. An exception would be if one of the two oxides could act as an internal catalyst,

providing more reactive species to the other oxide component, but in this case we would just deal with an extension of the use of noble metal additives. The case of the surface modification, instead, seems to introduce a novel material architecture, where the “upper” oxide provides charge carriers by faster and more efficient reactions with the gaseous analyte. On the other hand, the term “heterojunctions” becomes weaker since the surface layer is not really a crystalline structure, at least in our investigated samples, but resembles a distribution of monolayers.

This hybrid situation reflects itself in the choice of the sensing mechanism classification. In fact, the synergistic effect just described can then be ascribed to the surface-dependent class of mechanisms, mediated by catalytic effect, following Miller et al.[1]. Interestingly, those authors assigned this mechanism to decorated structures or mixed nanocrystalline systems. The case of core-shell systems, referred to *n-n* junctions, was classified in the group of surface sensitizations via carrier injection. The joining point between the two classifications, as concerns the present work, can be found if we consider the  $\text{WO}_x$  layer as a catalyst of the acetone combustion reactions. Thus, the surface layer is not simply acting as a metal oxide sensor but, in cooperation with the  $\text{TiO}_2$  substrate, can accelerate the acetone combustion. Such “cooperation” should be meant as a modified charge distribution in the  $\text{WO}_x$  layer as a consequence of the bonding with the underlying  $\text{TiO}_2$  core. Finally: what happens to the charge carriers generated by the reaction of acetone with the  $\text{WO}_x$  layer? Such carriers can be those previously trapped by chemisorbed oxygen, as classically supposed in gas-sensing mechanisms, or those provided by the any intermediate radical of the combustion reaction, but this is not the essential point. For fully understanding the operation mechanism, it is necessary to ascertain the following point: are they transported through a thin surface layer with enhanced conductance, or injected into the  $\text{TiO}_2$  core and then transported through the main conduction channel? The band structure of the two oxides [30] prescribes that electrons are injected from  $\text{TiO}_2$  to  $\text{WO}_3$ , which is opposite to what has been discussed until now. On the other hand, it is necessary to take into account that we do not have a crystal lattice of monoclinic  $\text{WO}_3$  onto the surface of anatase, but one or more layers for which a band structure cannot

be defined but at most a group of energy levels very different from bulk  $\text{WO}_3$ . A part of such levels may be present in the anatase gap, for instance due to the newly formed bonds on surface oxygen ions. This hypothesis would explain charge injection from the catalytic  $\text{WO}_x$  surface. On the other hand, despite the surface  $\text{WO}_x$  layers do not have the structure of bulk  $\text{WO}_3$ , they are still constituted by dense, corner sharing  $\text{WO}_6$  octahedra, resembling the structure of conductive  $\text{RhO}_3$  (to which bulk  $\text{WO}_3$  is related). Full understanding of this topic requires full understanding of the atomic structure of the surface layer, but will through light onto the complex sensing and conduction mechanisms of these materials.

#### **4. Conclusions**

The proper combination of the hydrolytic chemistry of Ti and W precursors resulted in different structures, depending on the W concentration. For lower W concentration, surface modification of the anatase nanocrystals by  $\text{WO}_x$  species occurred. For higher W concentration, heterojunctions were formed, where the presence of  $\text{WO}_3$  crystallites dispersed into the  $\text{TiO}_2$  host mainly contributed to conductance improvement. In both cases, a huge acetone response enhancement with respect to pure  $\text{TiO}_2$  was observed, at remarkably lower operating temperatures, clearly suggesting a catalytic effect due to the addition of the W oxide species.

#### **5. Acknowledgements**

Authors acknowledge CSIC/CNR project 2010IT0001 (SYNCAMON) and the SOLAR project DM19447. We thank Giovanni Battista Pace for the help with the sample preparation, and Nicola Poli for the help with the sensing measurements. A.G. acknowledges the funding from Generalitat de Catalunya 2014 SGR 1638, the Spanish MICINN project e-ATOM (MAT2014-51480-ERC) and the Turkish Ministry of National Education for the PhD scholarship. We also thank Jordi Arbiol for the additional HRTEM characterization.

#### **References**

[1] D.R. Miller, S.A. Akbar, P.A. Morris, Nanoscale metal oxide-based heterojunctions for gas sensing: A review, *Sens. Actuators, B*, 204 (2014) 250-272.


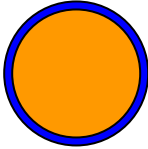
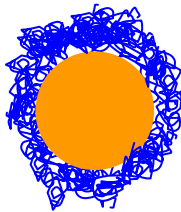

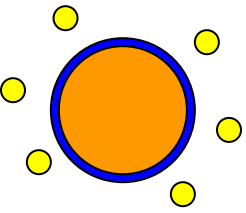
- [2] B. Lyson-Sypien, A. Czapla, M. Lubecka, E. Kusior, K. Zakrzewska, M. Radecka, A. Kusior, A.G. Balogh, S. Lauterbach, H.J. Kleebe, Gas sensing properties of TiO<sub>2</sub>-SnO<sub>2</sub> nanomaterials, *Sens. Actuators, B*, 187 (2013) 445-454.
- [3] M. Radecka, K. Zakrzewska, M. Rekas, SnO<sub>2</sub>-TiO<sub>2</sub> solid solutions for gas sensors, *Sens. Actuators, B*, 47 (1998) 194-204.
- [4] S. Morandi, G. Ghiotti, A. Chiorino, B. Bonelli, E. Comini, G. Sberveglieri, MoO<sub>3</sub>-WO<sub>3</sub> mixed oxide powder and thin films for gas sensing devices: A spectroscopic characterisation, *Sens. Actuators, B*, 111 (2005) 28-35.
- [5] L.Y. Chen, S.L. Bai, G.J. Zhou, D.Q. Li, A.F. Chen, C.L. Chung, Synthesis of ZnO-SnO<sub>2</sub> nanocomposites by microemulsion and sensing properties for NO<sub>2</sub>, *Sens. Actuators, B*, 134 (2008) 360-366.
- [6] B.P.J.D. Costello, R.J. Ewen, N. Guernion, N.M. Ratcliffe, Highly sensitive mixed oxide sensors for the detection of ethanol, *Sens. Actuators, B*, 87 (2002) 207-210.
- [7] S. Hemmati, A.A. Firooz, A.A. Khodadadi, Y. Mortazavi, Nanostructured SnO<sub>2</sub>-ZnO sensors: Highly sensitive and selective to ethanol, *Sens. Actuators, B*, 160 (2011) 1298-1303.
- [8] J.H. Yu, G.M. Choi, Electrical and CO gas sensing properties of ZnO-SnO<sub>2</sub> composites, *Sens. Actuators, B*, 52 (1998) 251-256.
- [9] G.N. Chaudhari, A.M. Bende, A.B. Bodade, S.S. Patil, V.S. Sapkal, Structural and gas sensing properties of nanocrystalline TiO<sub>2</sub> : WO<sub>3</sub>-based hydrogen sensors, *Sens. Actuators, B*, 115 (2006) 297-302.
- [10] S. Komornicki, M. Radecka, P. Sobas, Structural properties of TiO<sub>2</sub>-WO<sub>3</sub> thin films prepared by rf sputtering, *J. Mater. Sci.: Mater. Electron.*, 15 (2004) 527-531.
- [11] W.D. Lin, D.S. Lai, M.H. Chen, R.J. Wu, F.C. Chen, Evaluate humidity sensing properties of novel TiO<sub>2</sub>-WO<sub>3</sub> composite material, *Mater. Res. Bull.*, 48 (2013) 3822-3828.

- [12] K.O. Rocha, S.M. Zanetti, Structural and properties of nanocrystalline WO<sub>3</sub>/TiO<sub>2</sub>-based humidity sensors elements prepared by high energy activation, *Sens. Actuators, B*, 157 (2011) 654-661.
- [13] Y. Zhu, X.T. Su, C. Yang, X.Q. Gao, F. Xiao, J.D. Wang, Synthesis of TiO<sub>2</sub>-WO<sub>3</sub> nanocomposites as highly sensitive benzene sensors and high efficiency adsorbents, *J. Mater. Chem.*, 22 (2012) 13914-13917.
- [14] P. Rai, S.M. Majhi, Y.T. Yu, J.H. Lee, Noble metal@metal oxide semiconductor core@shell nano-architectures as a new platform for gas sensor applications, *RSC Adv.*, 5 (2015) 76229-76248.
- [15] M. Epifani, R. Díaz, C. Force, E. Comini, M. Manzanares, T. Andreu, A. Genç, J. Arbiol, P. Siciliano, G. Faglia, J.R. Morante, Surface Modification of TiO<sub>2</sub> Nanocrystals by WO<sub>x</sub> Coating or Wrapping: Solvothermal Synthesis and Enhanced Surface Chemistry, *ACS Appl. Mater. Interfaces*, (2015) 6898–6908.
- [16] M. Epifani, E. Comini, R. Díaz, T. Andreu, A. Genç, J. Arbiol, P. Siciliano, G. Faglia, J.R. Morante, Acetone Sensing with TiO<sub>2</sub>-WO<sub>3</sub> Nanocomposites: An Example of Response Enhancement by Inter-oxide Cooperative Effects, *Procedia Eng.*, 87 (2014) 803-806.
- [17] M. Epifani, E. Comini, G. Faglia, J. Arbiol, T. Andreu, G. Pace, P. Siciliano, J.R. Morante, Two step, hydrolytic-solvothermal synthesis of redispersible titania nanocrystals and their gas-sensing properties, *J. Sol-Gel Sci. Technol.*, 60 (2011) 254-259.
- [18] M. Epifani, T. Andreu, J. Arbiol, R. Diaz, P. Siciliano, J.R. Morante, Chloro-Alkoxide Route to Transition Metal Oxides. Synthesis of WO<sub>3</sub> Thin Films and Powders from a Tungsten Chloro-Methoxide, *Chem. Mater.*, 21 (2009) 5215-5221.
- [19] M. Epifani, E. Comini, R. Diaz, T. Andreu, A. Genc, J. Arbiol, P. Siciliano, G. Faglia, J.R. Morante, Solvothermal, Chloroalkoxide-based Synthesis of Monoclinic WO<sub>3</sub> Quantum Dots and Gas-Sensing Enhancement by Surface Oxygen Vacancies, *ACS Appl. Mater. Interfaces*, 6 (2014) 16808-16816.

- [20] D.B. Migas, V.L. Shaposhnikov, V.N. Rodin, V.E. Borisenko, Tungsten oxides. I. Effects of oxygen vacancies and doping on electronic and optical properties of different phases of  $\text{WO}_3$ , *J. Appl. Phys.*, 108 (2010).
- [21] R.D. Shannon, Revised effective ionic radii and systematic studies of interatomic distances in halides and chalcogenides, *Acta Crystallogr. Sect. A: Found. Crystallogr.*, 32 (1976) 751-767.
- [22] S.M. Zanetti, K.O. Rocha, J.A.J. Rodrigues, E. Longo, Soft-chemical synthesis, characterization and humidity sensing behavior of  $\text{WO}_3/\text{TiO}_2$  nanopowders, *Sens. Actuators, B*, 190 (2014) 40-47.
- [23] N. Izu, G. Hagen, F. Schubert, D. Schonauer-Kamin, R. Moos, Effect of a porous Pt/alumina cover layer for  $\text{V}_2\text{O}_5/\text{WO}_3/\text{TiO}_2$  resistive  $\text{SO}_2$  sensing materials, *J. Ceram. Soc. Jpn.*, 121 (2013) 734-737.
- [24] Y. Xie, R.Q. Xing, Q.L. Li, L. Xu, H.W. Song, Three-dimensional ordered ZnO-CuO inverse opals toward low concentration acetone detection for exhaled breath sensing, *Sens. Actuators, B*, 211 (2015) 255-262.
- [25] C. Su, Y.C. Zou, X.F. Xu, L. Liu, Z. Liu, L.L. Liu, Ultrahigh sensitivity of Nd-doped porous alpha- $\text{Fe}_2\text{O}_3$  nanotubes to acetone, *Colloid Surface A*, 472 (2015) 63-68.
- [26] A.K. Nayak, R. Ghosh, S. Santra, P.K. Guha, D. Pradhan, Hierarchical nanostructured  $\text{WO}_3\text{-SnO}_2$  for selective sensing of volatile organic compounds, *Nanoscale*, 7 (2015) 12460-12473.
- [27] Y.V. Kaneti, J.L. Moriceau, M. Liu, Y. Yuan, Q. Zakaria, X.H. Jiang, A.B. Yu, Hydrothermal synthesis of ternary alpha- $\text{Fe}_2\text{O}_3\text{-ZnO-Au}$  nanocomposites with high gas-sensing performance, *Sens. Actuators, B*, 209 (2015) 889-897.
- [28] C.H. Feng, X. Li, J. Ma, Y.F. Sun, C. Wang, P. Sun, J. Zheng, G.Y. Lu, Facile synthesis and gas sensing properties of  $\text{In}_2\text{O}_3\text{-WO}_3$  heterojunction nanofibers, *Sens. Actuators, B*, 209 (2015) 622-629.
- [29] F.D. Qu, J. Liu, Y. Wang, S.P. Wen, Y. Chen, X. Li, S.P. Ruan, Hierarchical  $\text{Fe}_3\text{O}_4@\text{Co}_3\text{O}_4$  core-shell microspheres: Preparation and acetone sensing properties, *Sens. Actuators, B*, 199 (2014) 346-353.

[30] N.M. Makwana, R. Quesada-Cabrera, I.P. Parkin, P.F. McMillan, A. Mills, J.A. Darr, A simple and low-cost method for the preparation of self-supported  $\text{TiO}_2\text{-WO}_3$  ceramic heterojunction wafers, *J Mater Chem A*, 2 (2014) 17602-17608.

**Table 1**

	Pure TiO <sub>2</sub>	R <sub>W</sub> = 0.16	R <sub>W</sub> = 0.64
<b>Cartoon</b>	 <p>Anatase nanocrystals (orange circle) all the way up to 500 °C</p>	 <p>All the way up to 500 °C: anatase coated with WO<sub>x</sub> layers (blue thick contour)</p>	 <p>As-prepared, amorphous WO<sub>x</sub> gel enwrapping the anatase nanocrystals;</p>   <p>At 500 °C WO<sub>3</sub> nanocrystals (yellow circles) segregate, the gel-like material is densified</p>
<b>XRD</b>	Anatase all the way up to 500 °C	Anatase all the way up to 500 °C	Anatase and amorphous WO <sub>x</sub> ; after 500 °C, anatase peak shift and WO <sub>3</sub> peaks
<b>Raman</b>	Anatase modes all the way up to 500 °C	Anatase modes and signal of WO <sub>x</sub> monolayers	Anatase and signal of WO <sub>x</sub> gel-like material; after heating at 500 °C, distorted anatase signal
<b>Electrical properties</b>	<i>n</i> type semiconductor	<i>n</i> type semiconductor, base conductance values comparable to pure TiO <sub>2</sub>	<i>n</i> type semiconductor, base conductance values about 100 times larger than pure TiO <sub>2</sub>

**Table 2**

<b>Material</b>	<b>Response to 25 ppm acetone<sup>*,**</sup></b>	<b>Operating temperature</b>	<b>Reference</b>
TiO <sub>2</sub> -WO <sub>3</sub> (R <sub>w</sub> = 0.16)	65	250 °C	This work
ZnO–CuO inverse opals	4.5 (20 ppm)	300 °C	24
Nd-doped α-Fe <sub>2</sub> O <sub>3</sub> nanotubes	22 (20 ppm)	240 °C	25
WO <sub>3</sub> -SnO <sub>2</sub>	>30 (1000 ppm)	300 °C	26
α-Fe <sub>2</sub> O <sub>3</sub> –ZnO	<20	225 °C	27
In <sub>2</sub> O <sub>3</sub> –WO <sub>3</sub> heterojunction nanofibers	8	275 °C	28
Fe <sub>3</sub> O <sub>4</sub> @Co <sub>3</sub> O <sub>4</sub> core– shell microspheres	<20	240 °C	29

\*: when the data for 25 ppm were not available, the closest concentration was considered instead;

\*\* : approximate values are reported, as obtained from the plotted data.

## Table captions

**Table 1:** cartoons depicting the main structural features of the prepared materials, and the related relevant structural and electrical features.

**Table 2:** comparison of the acetone responses obtained by various metal oxide nanocomposites.

## Figure Captions

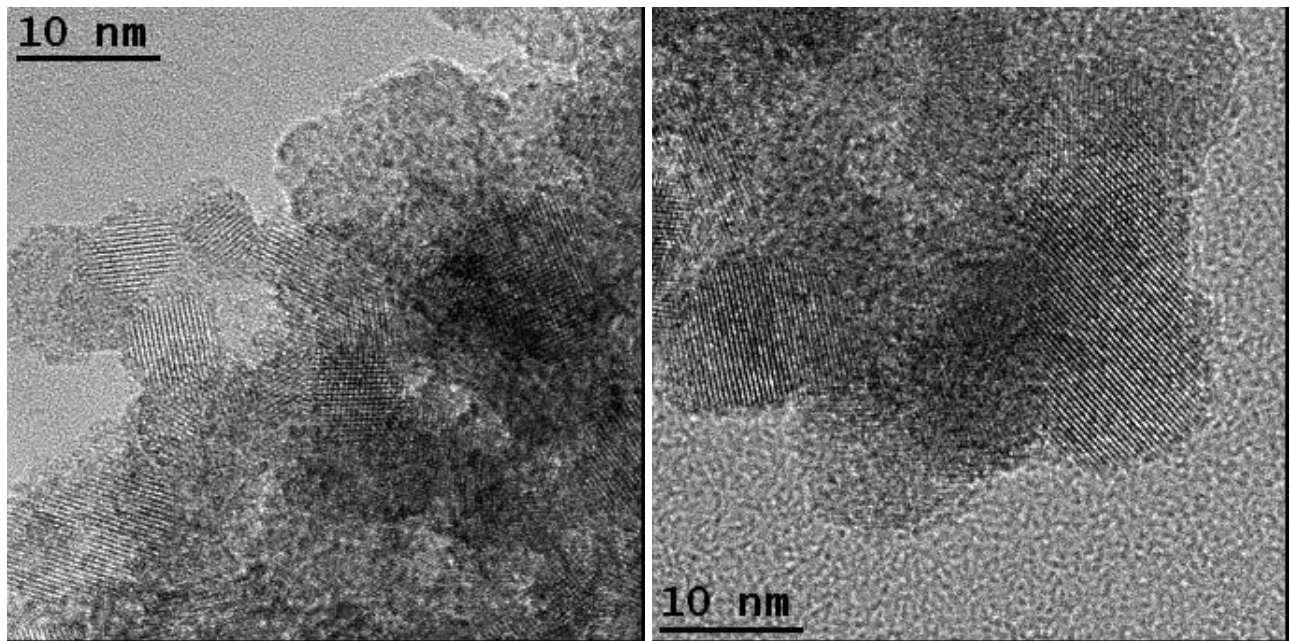
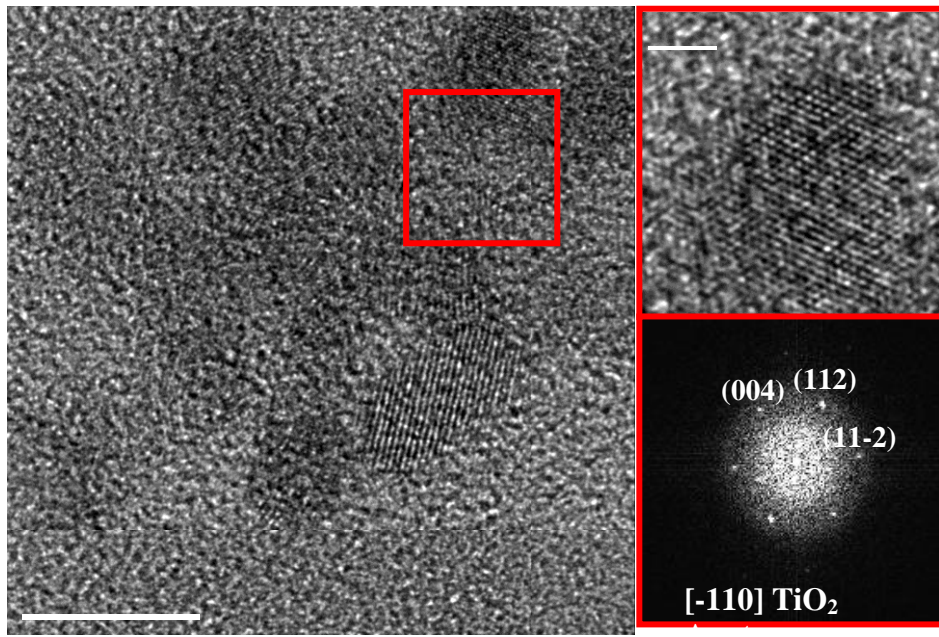
**Figure 1:** top: HRTEM images of the 500 °C (C)  $R_w = 0.16$  sample. The insets show magnifications of the red squared region, with the related power spectra; bottom: HRTEM image of the 500 °C  $R_w = 0.64$  sample.

**Figure 2:** Dynamic response of the indicated sensors towards acetone at an **operating** temperature of 250°C and 40% RH @20°C.

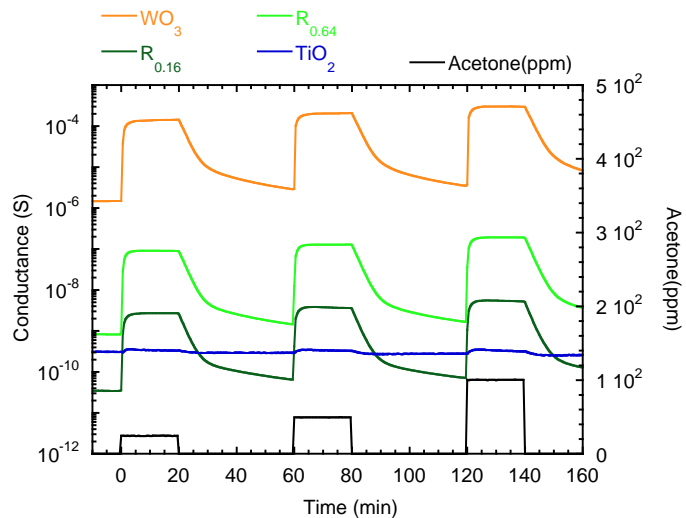
**Figure 3:** Calibration curve for acetone of the indicated sensors at an **operating** temperature of 250°C (left) and 400 °C (right) with 40% RH @20°C.

**Figure 4:** Response of the indicated sensors to 100 ppm of acetone as a function of the operating temperature.

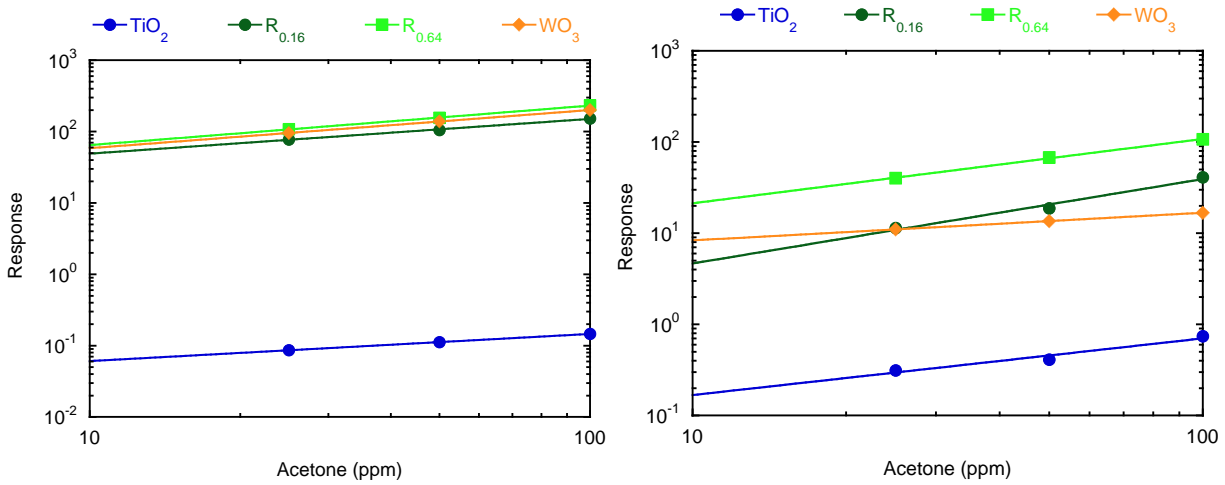
**Figure 5:** Response comparison at 200, 300 and 400 °C among NO<sub>2</sub> (5 ppm), H<sub>2</sub> (500 ppm), acetone (100 ppm) and ethanol (100 ppm).



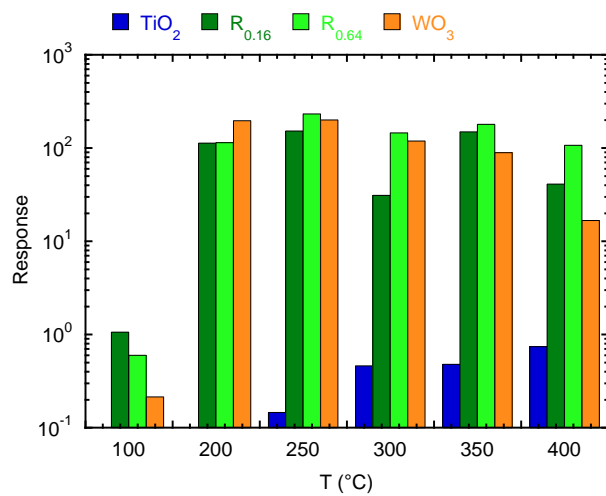
**Figure 1**



**Figure 2**



**Figure 3**



**Figure 4**

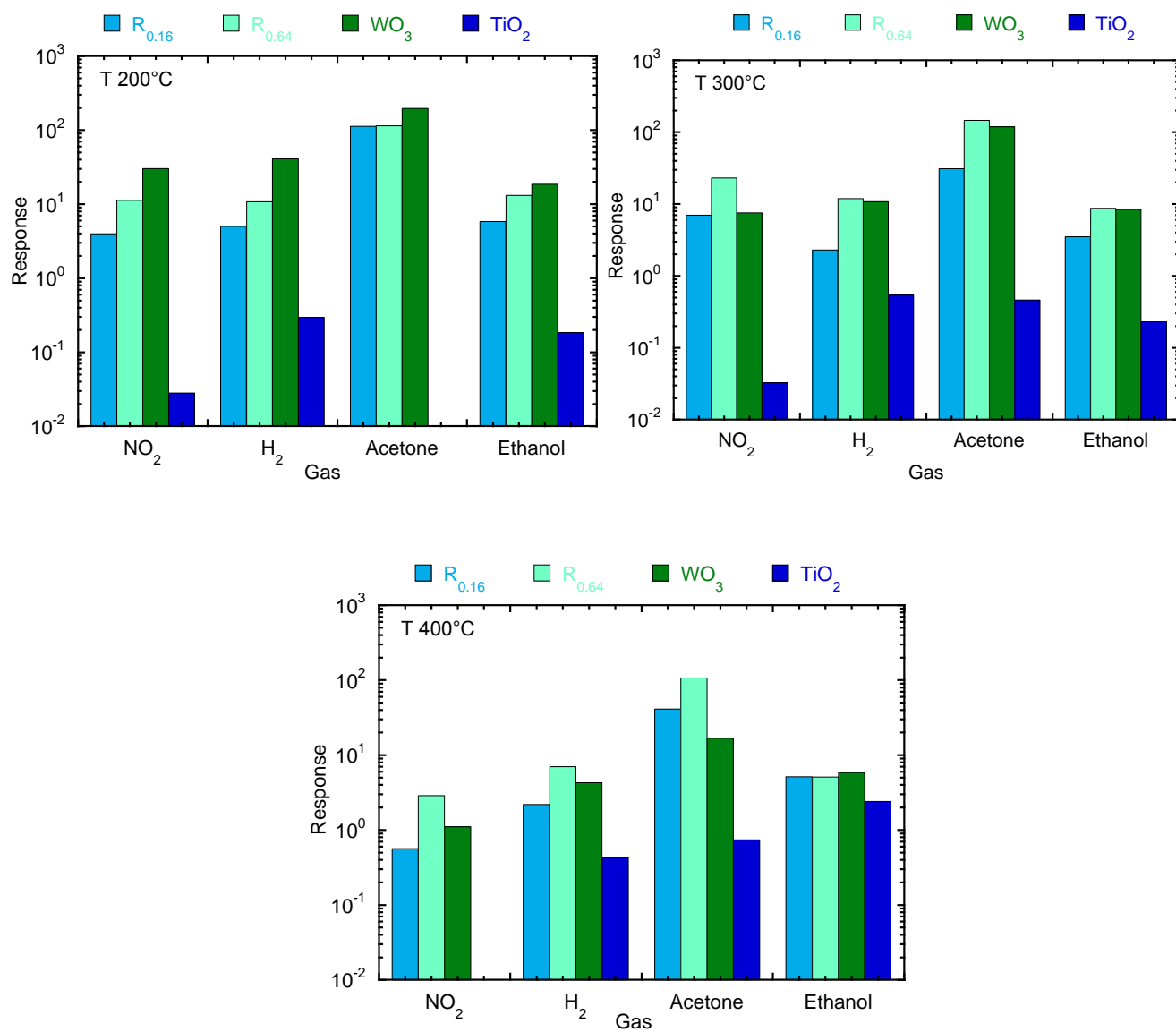


Figure 5

- Sensing architecture are synthesized, combining  $\text{WO}_3$  and of  $\text{TiO}_2$  nanocrystals.
- Surface layers of W oxides or heterojunctions of  $\text{TiO}_2$  and  $\text{WO}_3$  are obtained.
- Simple  $\text{TiO}_2$  surface modification by W oxides boosts the  $\text{TiO}_2$  acetone response.
- High responses even at 200 °C show catalytic effect of  $\text{WO}_3$  addition.

**Supplementary Material for on-line publication only**

[Click here to download Supplementary Material for on-line publication only: supplementary information.doc](#)